Moroccan Journal of Chemistry
ISSN: 2351-812X
http://revues.imist.ma/?journal=morjchem&page=login
xxxx / Mor. J. Chem. 6N°1 (2018) 22-34

Imidazo[4,5-b]pyridines as a New Class of Corrosion Inhibitors for Mild Steel: Experimental and DFT Approach

K. Bouayad[1,2], Y. Kandri Rodi[1], H. Elmsellem[3]*, E. H. El Ghadraoui[2], Y. Ouzidan[1], I. Abdel-Rahman[4], H.S. Kusuma[5], I. Warad[8], J.T. Mague[6], E.M. Essassi[7] and B. Hammouti[3],A.Chetouani[3]

[1]*Laboratory of Applied Organic Chemistry Sidi Mohamed Ben Abdellah University, Faculty of Sciences and Technology of Fez, Morocco*

[2]*Laboratoire de Chimie de la matière condensée, Faculté des Sciences et Techniques Université Sidi Mohamed Ben Abdallah, Fès Morocco*

[3]*Laboratoire de chimie analytique appliquée, matériaux et environnement (LC2AME), Faculté des Sciences, BP.717, 60000 Oujda, Morocco*

[4]*Department of Chemistry, College of Sciences, University of Sharjah, PO Box: 27272, UAE.*

[5]*Department of Chemical Engineering, Faculty of Industrial Technology, Institut Teknologi Sepuluh Nopember, 60111, Indonesia*

[6]*Department of Chemistry, Tulane University, New Orleans, LA 70118, USA*

[7]*Laboratoire de Chimie Organique Hétérocyclique, URAC, Université Mohamed V, Faculté des Sciences, Avenue Ibn-Batouta, Rabat, Morocco*

[8]*Department of Chemistry, AN-Najah National University P.O. Box 7, Nablus, Palestine*

** Corresponding author:*
h.elmsellem@gmail.com
Received 03 Jan 2017,
Revised 01 sept 2017,
Accepted 10 Sept 2017

Abstract

6-Bromo-2-methyl-1H-imidazo[4,5-b]pyridine (P1), was investigated for its adsorption and corrosion inhibition traits for mild steel corrosion in 1.0 M HCl solution. Gravimetric, potentiodynamic polarization and electrochemical impedance spectroscopy methods, were used to test the nature of adsorption and the inhibition effect of P1 on the mild steel in acidic media. It was found that the inhibition efficiency improved with the increase of P1 concentration in the acid solution (1.0 M HCl). The adsorption of P1 favored Langmuir adsorption isotherm. The results of corrosion tests confirmed that P1 could serve as an efficient corrosion inhibitor for the mild steel in 1.0 M HCl solution, yielding a high efficiency and low risk of environmental pollution. The theoretical quantum chemical calculations were in good correlation with the experimental results.

Keywords: *Imidazo[4,5-b]pyridines, Mild steel, Polarization, Electrochemical impedance spectroscopy, Quantum chemical calculations (DFT).*

1. Introduction

Mild steel with its relatively high strength, low cost, and widespread availability has been extensively utilized in numerous industrial applications such as petrochemical plants, power plants, oil and gas refineries, distillers, and ships[1-5]. However, low resistance of mild steel to acid corrosion has been the major hurdle in its applications, and therefore a need remains to prolong the lifetime of mild steel. Among the various approaches employed to minimize steel corrosion in acidic environment, the usage of inorganic/organic inhibitors is a well-established and cheapest method[6-10]. The inhibitors can be added to water tanks, pipeline streams, and so forth or incorporated into paint coatings, where they may form passive or almost impermeable films on the metal surface to reduce the rate of corrosion. Unfortunately, most of them are expensive, toxic toward the environment, and non-biodegradable. The adversely affecting chemicals and recent increase in environmental awareness have geared the research activities toward the development of nontoxic, cheap, environment-friendly, and biodegradable substances as inhibitors. Imidazo[4,5-b]pyridines are very useful intermediates/subunits for the development of molecules of pharmaceutical or biological interest. Imidazo[4,5-b]pyridine and its derivatives are an important class of bioactive molecules in the field of drugs and pharmaceuticals. Their activity includes antiviral anticancer, tituberculostatic and antimitotic actions [11-14]. They have also been evaluated as antagonists of various biological receptors including angiotensin-II [15]. Additionally, imidazo[4,5-b]pyridine derivatives have shown corrosion inhibition properties [16,17]. Hence, the synthesis of imidazo[4,5-b]pyridine derivatives represents nowadays an important topic in organic synthesis. The current work aims to study the effect of 6-Bromo-2-methyl-1H-imidazo[4,5-b]pyridine (P1) as environmentally friendly inhibitor for mild steel in 1.0 M HCl solution. Different methods such as potentiodynamic polarization, electrochemical impedance spectroscopy (EIS) and gravimetric measurements were used in this study.

2. Experimental

2.1. Synthesis of P1 Inhibitor

Dehydroacetic acid (3-acetyl-4-hydroxy-6-methyl-3H-pyran-2-one) (0.27 g, 1.6 mmol) was added to a solution of 5-bromopyridine-2,3-diamine (0.3 g, 1.6 mmol) in ethanol (15 ml) in a round bottomed flask. The mixture was refluxed for 24 hours. After the completion of reaction (as monitored by TLC), the crude product was obtained by suction filtration. The crude compound was recrystallized using a mixed solution of ethanol–water (1:1). The crystals obtained were colorless plates with a percentage yield equal to 68%, Scheme 1.

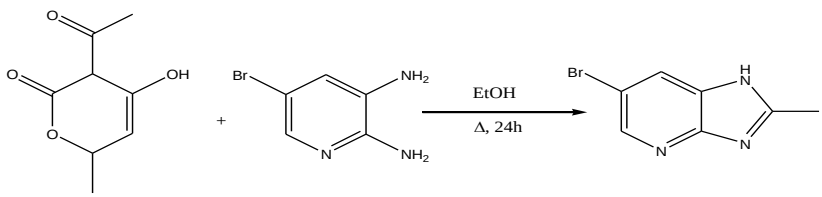

Scheme 1: Synthesis of 6-bromo-2-methyl-1H-imidazo[4,5-b]pyridine **P1.**

2.2. Materials

Mild steel specimens with composition (wt %) Fe 99.30%, C 0.076%, Si 0.026%, Mn 0.192%, P 0.012%, Cr 0.050%, Ni 0.050%, Al 0.023%, and Cu 0.135%, were polished using 600-1200 grade SiC Emery papers, washed with double distilled water, degreased with acetone in ultrasonic bath and finally allowed to dry in hot air. The gravimetric experiments were performed on mild steel specimens having dimension of 2.0 × 2.0 × 0.25 cm^3. On the other hand,

mild steel specimens with an exposed area of 1 cm^2 were used as working electrode for all electrochemical measurements. All the gravimetric and electrochemical experiments were performed in 1.0 M HCl solution. The 1.0 M HCl solutions were prepared by diluting the AR-grade HCl reagent (35%, MERCK) with double distilled water.

2.3. Gravimetric Measurements

The gravimetric experiments were performed as described previously [18]. All experiments were triply performed and the mean values were reported. Corrosion rate C_R (mg cm^{-2} h^{-1}) was calculated using the following relation:

$$C_{\mathrm{R}} = \frac{W}{At} \qquad \textbf{(1)}$$

Where, W is the average weight loss of three parallel mild steel strips, A is the exposed area of the strip and t is the immersion time (6 hours). From this calculated corrosion rate (C_R), the inhibition efficiency (η %) and surface coverage (θ) were calculated using the following relations:

$$\eta\% = \frac{C_{\mathrm{R}} - C_{\mathrm{R(i)}}}{C_{\mathrm{R}}} \times 100 \qquad \textbf{(2)}$$

$$\theta = \frac{C_{\mathrm{R}} - C_{\mathrm{R(i)}}}{C_{\mathrm{R}}} \qquad \textbf{(3)}$$

Where C_{R} and $C_{\mathrm{R(i)}}$ are the corrosion rate values for mild steel in 1.0 M HCl solutions in the absence and presence of different concentrations of P1 inhibitor, respectively.

2.4. Electrochemical Measurements

The conventional three electrode cell was used for electrochemical experiments. The mild steel specimens with a1 cm^2 exposed area as working electrode, high purity platinum as auxiliary electrode and saturated calomel electrode as reference electrode were used for electrochemical measurements. All the electrochemical experiments were performed with potentiostat PGZ 100 in 1.0 M HCl solutions in the absence and presence of different concentrations of P1 inhibitor after 30 minutes immersion time. Voltamaster software was used to analyze the experimental data derived from electrochemical studies. The EIS measurements were performed in frequency range of 100 kHz to 10 mHz under potentiodynamic condition having amplitude 10 mV peak to peak using AC signal at open circuit potential. From Nyquist plots, the charge transfer resistance (R_{ct}) values were calculated. Corrosion inhibition efficiency was calculated from the charge transfer resistance values using the following relationship:

$$\eta\% = \left(1 - \frac{R_{ct}}{R_{ct(i)}}\right) \times 100 \qquad \textbf{(4)}$$

Where, R_{ct} and $R_{\mathrm{ct(i)}}$ are the charge transfer resistance values in 1.0 M HCl solutions in the absence and presence of different concentrations of P1, respectively. The potentiodynamic polarization experiments were performed by automatic changing the electrode potential from −800 mV to −200 mV vs SCE (cathodic and anodic potential) with respect to open circuit potential at a sweep rate of 1 mV s^{-1}. The corrosion current densities (I_{corr}) were obtained by extrapolating the linear segment of the cathodic and anodic curves. From the corrosion current density, the inhibition efficiency was calculated using the following equation:

$$\eta\% = \left(1 - \frac{I_{\mathrm{corr(i)}}}{I_{\mathrm{corr}}}\right) \times 100 \qquad \textbf{(5)}$$

Where $I_{corr(i)}$ and I_{corr} are the corrosion current density values in 1.0 M HCl solutions without and with the presence of different concentrations of P1, respectively.

2.5. Computational Studies

Quantum chemical calculations are used to correlate the experimental data obtained for P1 inhibitor from different techniques (gravimetric measurements, potentiodynamic polarization and EIS) and its structural and electronic properties. Popular qualitative chemical concepts such as electronegativity [19, 20] (χ) and hardness [21] (η) have been provided with rigorous definitions within the purview of conceptual density functional theory [22-24] (DFT). Electronegativity is the negative of chemical potential defined [25] as follows for an N-electron system with total energy E and external potential $v(\vec{r})$:

$$\chi = -\mu = -\left(\frac{\partial E}{\partial N}\right)_{v(r)} \qquad \textbf{(6)}$$

Where, μ is the Lagrange multiplier associated with the normalization constraint of DFT [26, 27]. Hardness (η) is defined [28] as the corresponding second derivative as follows:

$$\eta = -\left(\frac{\partial^2 E}{\partial N}\right)_{v(r)} = -\left(\frac{\partial \mu}{\partial N}\right)_{v(r)} \qquad \textbf{(7)}$$

Using a finite difference method, working equations for the calculation of χ and η may be given by the following equations [29]:

$$\chi = \frac{I+A}{2} \qquad \textbf{(8)}$$

$$\eta = \frac{I-A}{2} \qquad \textbf{(9)}$$

Where, I = $-E_{HOMO}$ and A= $-E_{LUMO}$ are the ionization potential and electron affinity, respectively. Local quantities such as Fukui function *f*(r) defined the reactivity/selectivity of a specific site in a molecule. The Fukui function is defined as the first derivative of the electronic density q(r) of a system with respect to the number of electrons N at a constant external potential v(r) [30].

$$f(r) = \left[\frac{\partial \rho(r)}{\partial N}\right]_{v(r)} = \left[\frac{\delta \mu}{\delta v(r)}\right]_{N} \qquad \textbf{(10)}$$

Using left and right derivatives with respect to the number of electrons, electrophilic and nucleophilic Fukui functions for a site k in a molecule can be defined as follows [31]:

$$f_k^+ = P_k(N+1) - P_k(N) \quad for\ nucleophilic\ attack \qquad \textbf{(11)}$$

$$f_k^- = P_k(N) - P_k(N-1) \quad for\ electrphilic\ attack \qquad \textbf{(12)}$$

$$f_k^+ = [P_k(N+1) - P_k(N-1)]/2 \quad for\ radical\ attack \qquad \textbf{(13)}$$

where, $P_k(N)$, $P_k(N+1)$ and $P_k(N-1)$ are the natural populations for the atom k in the neutral, anionic and cationic forms, respectively. The fraction of transferred electrons ΔN was calculated according to Pearson theory [32]. This parameter evaluates the electronic flow in a reaction of two systems with different electronegativities, in particular case; a metallic surface (Fe) and an inhibitor molecule. ΔN is given as follows:

$$\Delta N = \frac{\chi_{Fe} - \chi_{inh}}{2(\eta_{Fe} + \eta_{inh})} \qquad \textbf{(14)}$$

Where, χ_{Fe} and χ_{inh} denote the absolute electronegativity of an iron atom (Fe) and an inhibitor molecule, respectively; η_{Fe} and η_{inh} denote the absolute hardness of Fe atom and the inhibitor molecule, respectively. In order to apply the eq. 12 in the present study, a theoretical value for the electronegativity of bulk iron was used $\chi Fe = 7$ eV and a global hardness of $\eta Fe = 0$, by assuming that for a metallic bulk I = A because they are softer than the neutral

metallic atoms [32]. The electrophilicity has been introduced by Parr et al. [33], which is a descriptor of reactivity that allows a quantitative classification of the global electrophilic nature of a compound within a relative scale. They have proposed the ω as a measure of energy lowering owing to maximize electron flow between donor and acceptor, which defined as follows:

$$\omega = \frac{\chi^2}{2\eta} \qquad \textbf{(15)}$$

The softness (σ) is defined as the inverse of the hardness (η) as follows [34]:

$$\sigma = \frac{1}{\eta} \qquad \textbf{(16)}$$

3. Results and discussion

3.1. Gravimetric Measurements

The corrosion values obtained from gravimetric measurements (Table 1), prove that (P1) acts as an efficient corrosion inhibitor for mild steel in 1.0 M HCl solution at 308 K. The inhibition efficiency increases with increasing (P1) concentration. The maximum inhibition efficiency value (94%) was obtained at a P1 concentration of 10^{-3}M at 308 K.

Table 1: The Corrosion rate and the inhibition efficiency values for mild steel in 1.0 M HCl solutions in the absence and presence of different concentrations of P1 inhibitor.

Concentration of P1 in 1.0 M HCl	**C_R (mg/cm^2 .h)**	**θ**	**η (%)**
--	0.826	--	--
10^{-6} M	0.192	0.77	77
10^{-5} M	0.106	0.87	87
10^{-4} M	0.065	0.92	92
10^{-3} M	0.049	0.94	94

The degree of protection against the acid attack is directly related to the area over the surface masked by the adsorption of P1. The number of the adsorbed P1 molecules on the surface of the mild steel increases with increasing P1 concentration, resulting in better protection. The surface coverage parameter, θ, defines the fraction of mild steel surface area that covered by the adsorbed P1 molecules on its surface.

3.2. Adsorption Isotherm

The surface coverage (θ) values obtained from the gravimetric measurements at 308 K were fitted to the various models of adsorption isotherms. It was found that the most accurate fit was the Langmuir adsorption isotherm, which represented in the following equation:

$$\frac{C}{\theta} = \frac{1}{\text{Kads}} + C \qquad \textbf{(17)}$$

Where, C is the concentration of P1 and K_{ads} is the adsorptive equilibrium constant. The plot of C/θ versus C (Figure 1) gives a straight line with a slope close to unity. The value of the slope as well as the linear correlation coefficients (R^2) were also close to unity, which indicates that P1 adsorption on the mild steel surface can be interpreted by the Langmuir adsorption isotherm. The higher the K_{ads} is ($7.31x0^5$ M^{-1}), the stronger and more stable adsorbed layer of P1 formed on the mild steel surface, which increases the inhibition efficiency. The adsorption equilibrium constant "K_{ads}", relative to standard adsorption free energy "ΔG_{ads}", is given by equation 18:

$\Delta G_{ads} = -RT.ln(55.5K_{ads})$ **(18)**

where 55.5 represents the water concentration (mol L^{-1}) in solution. The values of ΔG_{ads} obtained up to −20 kJ mol^{-1}, generally, are indicative of the electrostatic interaction between the charged metal and a charged inhibitor molecules, that is, physisorption, whereas those equal to or more in negative value than −40 kJ mol^{-1}, suggest the formation of coordinate bonds through sharing or relocation of charge from P1 molecules to the mild steel surface, which implies chemisorption. In the present study, the $\Delta G°_{ads}$ value obtained for the (P1) inhibitor on mild steel in 1.0 M HCl solution is -44.86 kJ mol^{-1}. Therefore, it is concluded that chemisorption interactions should be dominant for the adsorption of the P1 molecules on the mild steel surface [37].

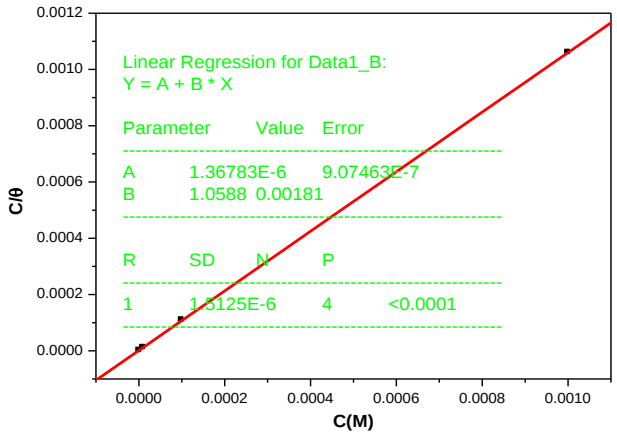

Figure 1: The plot of (C/θ) versus the concentration of P1 (C) for mild steel in 1.0 M HCl solution at 308 K obtained from gravimetric measurements.

3.3. Electrochemical measurements

3.3.1 Electrochemical impedance spectroscopy (EIS)

The corrosion of mild steel in 1.0 M HCl solution in the presence of P1 was investigated by EIS at 308 K after an exposure period of 1/2 h at OCP. Nyquist plots for mild steel obtained at the interface in the absence and presence of various concentrations of P1 is given in Figure 2. The Nyquist plots show semicircles with single capacitive loop and increasing diameter as the concentration of the P1 increases. Deviations from a perfect circular shape indicate frequency dispersion of interfacial impedance arising from lack of homogeneity of the electrode surface due to roughness or interfacial phenomenon [38, 39]. That is why the pure capacitance is substituted by a Constant Phase Element (CPE), i.e., a model element of frequency distributed behavior is introduced to the structural model illustrated in Figure 3. CPE summarizes the impedance answer of the distribution process in a single expression given by [40]:

$$Z_{CPE} = \frac{1}{A}(j\omega)^{-n} \qquad \textbf{(19)}$$

Where, Z_{CPE} is the impedance of CPE, A is the CPE constant, ω is the angular frequency, j is the imaginary unit $(-1)^{1/2}$, and n has the meaning of a phase shift. CPE has pure capacitance behavior in case n =1. The dispersion of the capacitance semicircle is usually connected with surface inhomogeneity, active centers distribution, inhibitor adsorption, formation of porous layers, etc. [40–43].

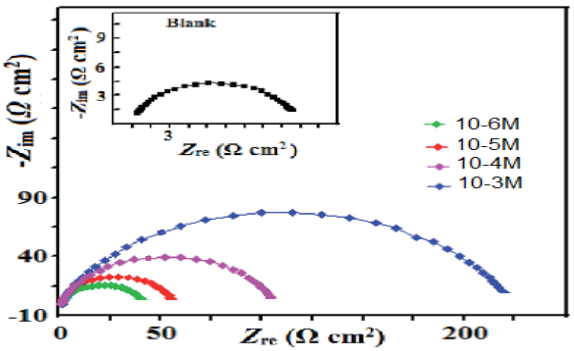

Figure 2: Electrochemical impedance spectra (Nyquist plots) of mild steel in 1.0 M HCl solution without and with different concentrations of P1 at 308 K.

The capacitance values of the electrical double layer were calculated according to the following equation [44, 45]:

$$C_{dl} = \left(AR_{ct}^{1-n}\right)^{\frac{1}{n}} \qquad \textbf{(20)}$$

Where, A is the magnitude of CPE, Rct is the charge transfer resistance, and n is the CPE exponent. Simulation of Nyquist plots with Randle's model (Figure 3) containing constant phase element (CPE) instead of capacitance and charge transfer resistance (Rct), showed excellent agreement with experimental data. The main parameters deduced from the analysis of Nyquist diagram for 1.0 M HCl solution without and with P1 is given in Table 2. By increasing P1 concentration from 10^{-6}M to 10^{-3}M, the charge transfer resistance (R_{ct}) increased and the capacitance (C_{dl}) decreased, indicating that increasing P1 concentration decreased the corrosion rate. The decrease in the capacitance was caused by reduction in local dielectric constant and/or by the increase in thickness of the electrical double layer. This fact suggests that the inhibitor molecules acted by adsorption at the mild steel/solution interface [46–48]. On the other hand the decrease in C_{dl} with the increase in concentration of P1 was a result of the increase in the surface coverage (θ) by the inhibitor, which led the increase in the inhibition efficiency. The thickness of the protective layer, δ_{org}, was related to C_{dl} by the following equation (21). Where ε_0 is the dielectric constant and ε_r is the relative dielectric constant.:

$$\delta_{org} = \frac{\varepsilon_0 \varepsilon_r}{C_{dl}} \qquad \textbf{(21)}$$

Table 2: Impedance parameters for mild steel corrosion in 1.0 M HCl solution without and with different concentrations of P1 at 308 K.

Inhibitor in 1.0 M HCl	Conc (M)	R_s (Ω)	R_{ct} (Ω cm^2)	n	A (μFcm^{-2})	C_{dl} (μFcm^{-2})	θ	η %
--	--	1.15	10	0.82	249	200	--	--
P1	10^{-6}	0.80	74	0.81	197	94	0.86	86
	10^{-5}	1.25	108	0.84	172	89	0.91	91
	10^{-4}	1.21	175	0.89	142	80	0.94	94
	10^{-3}	1.35	271	0.87	137	55	0.96	96

Since adsorption of an organic inhibitor on a metal surface involves the replacement of water molecules and other ions originally adsorbed on the mild steel surface, the smaller dielectric constant of organic compounds compared to water as well as the increased thickness of the double layer due to inhibitor adsorption act simultaneously to reduce the interfacial capacitance [49–51]. This provides experimental evidence of adsorption of the P1 molecules on the mild steel surface.

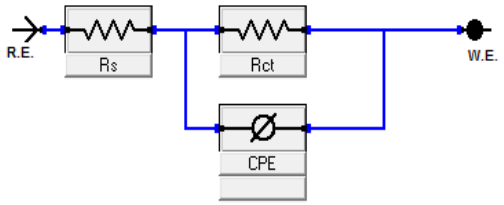

Figure 3: Equivalent circuit model represents the metal/solution interface: CPE is the constant phase element, Rct is the charge transfer resistance and RS is the resistance of solution

3.3.2. Polarization Measurements

Potentiodynamic polarization curves for mild steel in 1.0 M HCl solution containing different concentrations of P1 is shown in Figure 4. It is clearly noticed from Figure 4, that both the cathodic anodic reactions are inhibited and the inhibition increased as the inhibitor concentration increased.

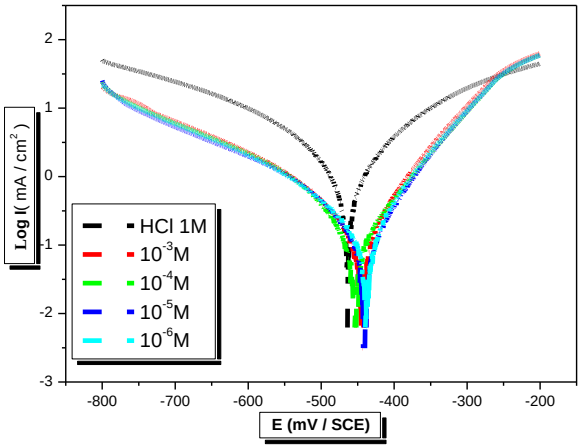

Figure 4: Potentiodynamic polarization curves of mild steel in 1.0 M HCl solution without and with various concentrations of P1 at 308 K.

T**able 3:** Polarization parameters for mild steel corrosion in 1.0 M HCl solution without and with various concentrations of P1 at 308 K.

Inhibitor in 1.0 M HCl	Concentration of Inhibitor (M)	$-E_{corr}$ (mV/SCE)	$-\beta_c$ (mV/dec)	I_{corr} (mA/cm^2)	η (%)
--	--	467	187	1386	--
P1	10^{-6}	461	129	271	80
	10^{-5}	466	131	208	85
	10^{-4}	463	107	134	90
	10^{-3}	462	172	94	93

The respective kinetic parameters obtained from Figure 4 are given in Table 3. The values given in the Table 3 show that the corrosion current (I_{corr}) decreased markedly in the presence of P1 and the magnitude of change increases with increasing P1 concentration. This confirms the inhibitive action of the P1 in the 1 M HCl medium. With increase in P1 concentration, the corrosion potential (E_{corr}) did not vary much. The values of both anodic and cathodic Tafel constants βa and βc respectively are markedly changed in the presence of the P1. This confirms the mixed mode of inhibition of the P1 inhibitor.

3.3. Quantum Chemical Calculations

The FMOs (HOMO and LUMO) are very important for describing chemical reactivity. The HOMO containing electrons, represents the ability (E_{HOMO}) to donate an electron, whereas, LUMO haven't not electrons, as an electron acceptor represents the ability (E_{LUMO}) to obtain an electron. The energy gap between HOMO and LUMO determines the kinetic stability, chemical reactivity, optical polarizability and chemical hardness–softness of a compound [35]. In this study, the HOMO and LUMO orbital energies were calculated using B3LYP method with 6-31G(d,p). All other calculations were performed using the results with some assumptions. The higher values of E_{HOMO} indicate an increase for the electron donor of the studied P1 inhibitor and this means a better inhibition corrosion efficiency with increasing adsorption of the P1 inhibitor molecules on the mild steel surface, whereas E_{LUMO} indicates the ability of the P1 molecules to accept electrons. The adsorption ability of the inhibitor to the metal surface increases with increasing of E_{HOMO} and decreasing of E_{LUMO}. The HOMO and LUMO energies as well as other parameters were shown in Table 4.High ionization energy (I= 6.29 eV) indicates high stability, the number of electrons transferred (ΔN) was also calculated and tabulated in Table 4. The ΔN value was 0.6365, ($\Delta N < 1.6$), which indicates the tendency of P1 molecules to donate electrons to the metal surface.

Table 4: Quantum chemical parameters for P1 obtained in gaseous phase using the DFT at the B3LYP/6-31G level

Parameter	**Value**
Total Energy *TE* (eV)	-81802.5
E_{HOMO} (eV)	-6.2961
E_{LUMO} (eV)	-1.1390
Gap ΔE (eV)	5.1571
Dipole moment (μ in Debye)	5.7246
Ionization potential (I in eV)	6.2961
Electron affinity (A)	1.1390
Electronegativity (χ)	3.7176
Hardness (η)	2.5786
Electrophilicity index (ω)	2.6799
Softness (σ)	0.3878
Fractions of electron transferred (ΔN)	0.6365

The calculated values of the f_k^+ for the P1 inhibitor are mostly localized on the pyridine ring (Table 5). Namely C_3, N_1 and Br_1, indicating that the pyridine ring may be probably the favorite site for nucleophilic attack. The results also show that Br_{13} atom is suitable site to undergo both nucleophilic and electrophilic attacks, probably allowing them to adsorb easily and strongly on the mild steel surface. The final optimized geometry and Ortep representation obtained

from X-ray diffraction of compound **P1** [36] are shown in Figures 5 and 6 respectively. As clearly shown in Figure 6, P1 crystallizes in two forms, A and B, in two asymmetric units, with all non-hydrogen atoms lying on a crystallographic mirror plane. A DFT calculation was carried out to predict the geometry of the P1 molecules.

Table 5: Pertinent natural populations and Fukui functions of **P1** calculated at B3LYP/6-31G in the gaseous phase.

Atom	P(N)	P(N-1)	P(N+1)	f^-	f^+	f^0
C3	6,2784	6,4240	6,2476	0,1456	0,0308	0,0882
C6	5,5577	5,7020	5,4509	0,1443	0,1068	0,1255
Br1	34,9296	35,0837	34,6633	0,1541	0,2664	0,2102
N1	7,4280	7,5624	7,3806	0,1345	0,0474	0,0909

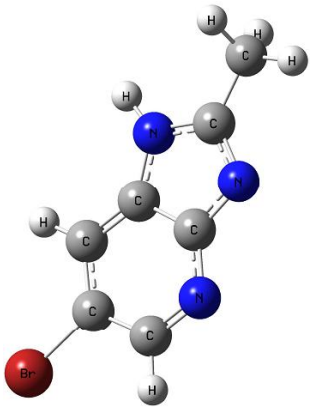

Figure 5: optimized structure of **P1**

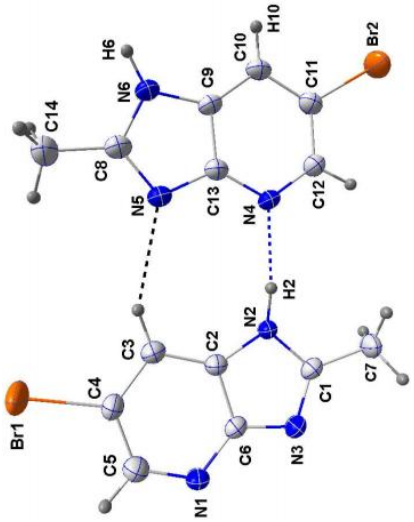

Figure 6: Ortep representation of Asymmetric unit with 50% probability ellipsoids.

The selected actual and optimized bond lengths and bond angles obtained by X-ray crystallographic study as well as by geometry optimization at B3LYP/6-31G level of theory of structure P1 are reported in Tables 6 and 7, respectively.

Table 6: Selected X-ray and calculated bond lengths (Å) of inhibitor **P1**

Entry	**X-ray (A)**	**Entry**	**X-ray (B)**	**Calculated**
Br1—C4	1.899 (3)	Br2—C11	1.901 (3)	1.8513
N1—C5	1.326 (4)	N4—C12	1.335 (4)	1.3058
N1—C6	1.333 (4)	N4—C13	1.344 (4)	1.3567
N2—C1	1.365 (4)	N6—C8	1.363 (4)	1.3792
N2—C2	1.367 (4)	N6—C9	1.375 (4)	1.3713
N3—C1	1.313 (4)	N5—C8	1.329 (4)	1.3446
N3—C6	1.372 (4)	N5—C13	1.376 (4)	1.3375
C1—C7	1.488 (4)	C8—C14	1.480 (5)	1.4779
C2—C3	1.383 (4)	C9—C10	1.384 (4)	1.3788
C2—C6	1.425 (4)	C9—C13	1.409 (4)	1.4592
C3—C4	1.378 (5)	C10—C11	1.389 (4)	1.4028

Table 7: Selected X-ray and calculated bond angles (°) of inhibitor **P1**

Entry	X-ray (A)	Entry	X-ray (B)	Calculated
C1—N2—C2	106.8 (3)	C8—N6—C9	106.7 (3)	107.34
C1—N3—C6	104.6 (2)	C8—N5—C13	104.1 (3)	105.58
N3—C1—N2	113.8 (3)	N5—C8—N6	113.5 (3)	112.42
N3—C1—C7	125.2 (3)	N5—C8—C14	124.8 (3)	124.62
N2—C1—C7	120.9 (3)	N6—C8—C14	121.6 (3)	122.95
N2—C2—C3	134.7 (3)	N6—C9—C10	133.3 (3)	134.68
N2—C2—C6	104.8 (3)	N6—C9—C13	105.0 (3)	103.93
N1—C6—N3	126.6 (3)	N4—C13—N5	125.8 (3)	125.71
C4—C3—C2	114.2 (3)	C9—C10—C11	113.6 (3)	113.86
C3—C4—Br1	118.8 (2)	C10—C11—Br2	119.3 (2)	120.76

The experimental and calculated DFT, B3LYP bond lengths of all atoms in the compound **P1** were correlated nicely (the differences are between 0.01～0.05 Å). About 0.02～ 2º differences in the bond angles were found between the experimental and theoretical values.

4. Conclusion

It was found that P1 is an efficient corrosion inhibitor for mild steel in 1.0 M HCl. Polarization studies showed that P1 was a mixed-type inhibitor and its inhibition efficiency increased with the increase of inhibitor concentration. Data obtained from ac impedance technique show a frequency distribution and therefore a modeling element with frequency dispersion behavior, using a constant phase element (CPE). The inhibition efficiency values, calculated from the electrochemical impedance spectroscopy study, show the same trend as those obtained from the potentiodynamic polarization curves measurements. The adsorption of P1 molecules on the mild steel surface in 1.0 M HCl solution obey Langmuir adsorption isotherm with high correlation coefficient. Experimental results were supported by DFT-based quantum chemical calculations. Several derived DFT-based parameters such as E_{HOMO}, E_{LUMO}, ΔE, χ, σ, η, and ΔN of the P1 inhibitor validated the experimentally determined values of the inhibition efficiency.

References

[1] H. Elmsellem, T. Harit, A. Aouniti, F. Malek, A. Riahi, A. Chetouani, B. Hammouti, Protection of Metals and Physical Chemistry of Surfaces. 51 (2015) 873–884.

[2] H. Elmsellem , H.Nacer, F.Halaimia, A.Aouniti, I.Lakehal, A.Chetouani, ,Int. J. Electrochem. Sci, 9 (2014) 5328-5351.

[3] A. Aouniti, H. Elmsellem, S. Tighadouini, Journal of Taibah University for Science, (2015), http://dx.doi.org/10.1016/j.jtusci.2015.11.008.

[4] H. Elmsellem, N. Basbas, A. Chetouani, A. Aouniti, Portugaliae. Electrochimica Acta, 2 (2014) 77-108.

[5] H. Elmsellem, K. Karrouchi, Der PharmaChemica, 7 (2015) 237-245.

[6] H. Elmsellem , M. H. Youssouf, A. Aouniti, Russian, Journal of Applied Chemistry. 8 (2014) 744−753.

[7] Y. El Ouadi, Lahhit, N., Bouyanzer, A. Elmsellem, H., Majidi, L., Znini, M., Abdel Rahman, I., Hammouti, B., El Mahi, B. and Costa, J. International Journal of Development Research,6 (2016) 6867-6874.

[8] H. Elmsellem, AounitiA., YoussoufiM.H., BendahaH., Ben hadda T., Chetouani A., Warad I., Hammouti B., Phys. Chem. News, 70 (2013) 84.
[9] H. Elmsellem, Elyoussfi A., Sebbar N. K., Dafali A., Cherrak K., Steli H., Essassi E. M., Aouniti A. and Hammouti B., Maghr. J. Pure & Appl. Sci, 1 (2015) 1-10.
[10] H. Elmsellem, Aouniti A.,Khoutoul M., Chetouani A., Hammouti B., Benchat N.,Touzani R. and Elazzouzi M., J. Chem. Pharm. Res, 6 (2014) 1216.
[11] G. Aridoss, S. Balasubramanian, P. Parthiban, and S. Kabilan, Eur. J Med. Chem. 41 (2006) 268–275.
[12] V. Bavetsias, C. Sun, N. Bouloc, J. Reynisson, P. Workman,S. Linardopoulos and E. McDonald, Bioorg. Med. Chem. Lett. 17 (2007) 6567–6571.
[13] L. Bukowski, and R. Kaliszan, Arch. Pharm. 324 (1991) 121–127.
[14] G. Cristalli, S. Vittori, A. Eleuteri, R. Volpini, E. Camaioni,G. Lupidi, N. Mahmood, F. Bevilacqua, and G. Palu, J. Med. Chem. 38 (1995) 4019–4025.
[15] Chen, S. T. and Dost, G. US Patent 1992, 5 ,132-216
[16] M. Sikine, H. Elmsellem, Y. Kandri Rodi, H. Steli, A. Aouniti, B. Hammouti, Y. Ouzidan, F. Ouazzani Chahdi, M. Bourass, and E. M. Essassi, J. Mater. Environ. Sci. 7 (2016) 4620-4632.
[17] S. Bourichi, Y. Kandri Rodi, H. Elmsellem, H. Steli, Y. Ouzidan, N. K. Sebbar, F. Ouazzani Chahdi, E. M. Essassi, F. El-Hajjaji and B. Hammouti, Der Pharma Chemica, 8 (2016) 179-186.
[18] H. Elmsellem, Elyoussfi A., Steli H., Sebbar N. K., Essassi E. M., Dahmani M., El Ouadi Y., Aouniti A., El Mahi B., Hammouti B., Der Pharma Chemica,8 (2016) 248-256.
[19] L. Pauling, The nature of the chemical bond, 3rd edn. Cornell University Press, Ithaca, 1960.
[20] K.D. Sen and C. Jorgenson, Structure and bonding: electronegativity, Springer, Berlin, 1987, 66.
[21] K.D. Sen and D.M.P. Mingos, Structure and bonding: chemical hardness, Springer, Berlin, 1993, 80.
[22] R.G. Parr and W. Yang, Density functional theory of atoms and molecules, Oxford University Press, Oxford, 1989.
[23] P. Geerlings, F. de Proft and W. Langenaeker, Chem. Rev., 103 (2003) 1793-1873.
[24] H. Chermette, J. Comput. Chem., 20 (1999) 129-154.
[25] R.G. Parr, R.A. Donnelly, M. Levy and W. Palke, J. Chem. Phys., 68 (1978) 3801-3807.
[26] P. Hohenberg, Kohn, Phys. Rev. B., 136 (1964) 864-871.
[27] W. Kohn and L. Sham, J. Phys. Rev. A., 140 (1965) 1133.
[28] R.G. Parr and R.G. Pearson, J. Am. Chem. Soc., 105 (1983) 7512-7516.
[29] I. B. Obot and N. O. Obi-Egbedi, Corrosion Science, 52 (2010) 657-660.
[30] W. Yang and W. Mortier, J. Am. Chem. Soc., 108 (1986) 5708-5711.
[31] R.K. Roy and S. Pal, K. Hirao, J. Chem. Phys., 110 (1999) 8236-8245.
[32] R.G. Pearson, Inorg. Chem., 27 (1988) 734-740.
[33] V.S. Sastri and Perumareddi, J.R., Corrosion, 53 (1997) 671.
[34] P. Udhayakala, T. V. Rajendiran, and S. Gunasekaran, Journal of Chemical, Biological and Physical Sciences A, 2 (2012) 1151-1165.
[35] M. Govindarajan, M. Karabacak, Spectrochim Acta Part A Mol Biomol Spectrosc, 85 (2012) 251–260
[36]K. Bouayad, Y. Kandri Rodi, E. H. El Ghadraoui, J. T. Mague, E. M. Essassi and H. Zouihri, IUCrData , 2016, 160766.
[37] I. Chakib, H. Elmsellem, Sebbar N. K., Lahmidi S., Nadeem A., Essassi E. M., Ouzidan Y., Abdel-Rahman I., Bentiss F., B. Hammouti., J. Mater. Environ. Sci, 7 (2016) 1866-1881.

[38] H. Darmokoesoemo, H.Setyawati, A. T .A. Ningtyas,Y. Kadmi, H. Elmsellem, Heri Septya Kusuma. Results in Physics. http://dx.doi.org/10.1016/j.rinp.2017.08.009
[39] R.Chadli, Elazouzi M., Khelladi I., Elhourri A.M., H. Elmsellem, Aouniti A., Kajima Mulengi J., Hammouti B., Portugaliae Electrochimica Acta. 35 (2017) 65-80.
[40] Y. El Ouadi, M. Manssouri, A. Bouyanzer, H. Bendaif, H. Elmsellem, B. Hammouti, Microbial Pathogenesis .107 (2017) 1-6.
[41] Z.Tribak, Y. Kandri Rodi, H. Elmsellem, J. Mater. Environ. Sci. 8 (2017) 1116 -1127.
[42] H. Bendaha, H. Elmsellem, A. Aouniti, M. Mimouni, A.Chetouani, B. Hammouti, Physicochemical Mechanics of Materials. 1 (2016) 111-118.
[43] A. Elyoussfi, A. Dafali, H. Elmsellem, H. Steli, Y. Bouzian Y, J. Mater. Environ. Sci. 7 (2016) 3344-3352.
[44] M. Ramdani, H. Elmsellem, N. Elkhiati, B.Haloui, A. Chetouani and B. Hammouti , Der Pharma Chem.7 (2015) 67-76.
[45] N. K.Sebbar, H. Elmsellem, M. Boudalia, S. lahmidi , A. Belleaouchou, A. Guenbour, H. Steli H., J. Mater. Environ. Sci. 6 (2015) 3034-3044.
[46] S.Lahmidi, H. Elmsellem, A. Elyoussfi, N. K. Sebbar, Y. Ouzidan, Y. KandriRodi , and B. Hammouti, Der Pharma Chemica. 8 (2016) 294-303.
[47] M. Y.Hjouji, M.Djedid, H. Elmsellem, Kandri Rodi Y., Benalia M., Steli H., Ouzidan Y., Ouazzani Chahdi F., Essassi E. M., Hammouti B., Der Pharma Chemica. 8 (2016) 85-95.
[48] Y. Filali Baba, H. Elmsellem, Y. KandriRodi, H. Steli , Y. Ouzidan , F. Ouazzani Chahdi, Der Pharma Chemica. 8 (2016)159-169.
[49] Z.Tribak, Y.Kandri Rodi, H. Elmsellem, I. Abdel-Rahman, A. Haoudi, M. K. Skalli, J. Mater. Environ. Sci. 8 (2017) 1116 -1127.
[50] G. Aziate, H. Elmsellem, N.K. Sebbar, Y. El Ouadi, J. Mater. Environ. Sci, 8 (2017) 3873-3883.
[51] K. Abdu, N. K. Sebbar, H. Elmsellem, N. Abad, DahdouhA., E. M. Essassi, Y. Ouzidan, J. Mater. Environ. Sci., 8 (2017) 4160-4170
[52] A. Zouitini, Y. Kandri Rodi, H. Elmsellem, H. Steli, F. Ouazzani Chahdi, Y. Ouzidan, N. K. Sebbar, E. M. Essassi, F. El-Hajjaji and B. Hammouti, Der Pharma Chemica. 8 (10) (2016) 23-31.